

Bose-Einstein Condensation and the Lambda Transition for Interacting Lennard-Jones Helium-4

Phil Attard
 phil.attard1@gmail.com October 7, 2025

An introduction to Bose-Einstein condensation and the λ -transition is given. Results of quantum loop Monte Carlo simulations are presented for interacting Lennard-Jones helium-4. The optimum condensation fraction is found by minimizing the constrained free energy. The results show that approaching the transition the growth of pure position permutation loops and the consequent divergence of the heat capacity are enabled by the suppression of condensation and consequently of superfluidity. Condensation and superfluidity emerge at the peak of the heat capacity due to mixed position permutation chains.

I. INTRODUCTION

In the fields of superfluidity and the λ -transition there are several important questions that have received little attention. First, what suppresses Bose-Einstein condensation above the λ -transition? After all, if, as conventional wisdom asserts, Bose-Einstein condensation is bosons in the ground energy state, its very hard to see why there are *no* bosons in the ground energy state above the λ -transition. Yet this must be the case if superfluidity is carried by condensed bosons because superfluidity is not observed above the λ -transition.

Second, why does the heat capacity diverge, and why does it do so over such a narrow temperature range (about 0.4 K)? In the widely accepted non-interacting boson analysis of Bose-Einstein condensation and the λ -transition, the peak of the heat capacity is finite (Attard 2025a, Le Bellac *et al.* 2004, F. London 1938, Pathria 1972). Thus the measured divergence must be due to interactions between the atoms. It remains to give the molecular structure causing it and to explain why it occurs over such a narrow range.

And third, why does this divergence in the heat capacity coincide with the onset of superfluidity? It is as if the divergence itself catalyzes condensation and overcomes the previous suppression, but it is difficult to understand this at the molecular level.

This paper answers these questions using quantum loop Monte Carlo simulations of Lennard-Jones ${}^4\text{He}$, guided by existing experimental observations.

A. Background

I take it as axiomatic

- that the λ -transition and superfluidity in liquid helium-4 are due to Bose-Einstein condensation
- that a condensed boson is one in a highly occupied momentum state.

The λ -transition is signified by a spike in the heat capacity of saturated liquid ${}^4\text{He}$ at 2.2 K. The experimental

evidence is that on the liquid saturation curve the energy, the density, and the shear viscosity are continuous functions of temperature at the λ -transition; the density and the shear viscosity have a discontinuity in their first temperature derivative (Donnelly and Barenghi 1998). The heat capacity has an integrable divergence at the λ -transition (Lipa *et al.* 1996). Superfluid flow occurs in thin films and capillaries immediately below the λ -transition, but not above it.

In so far as superfluidity is due to Bose-Einstein condensation, the first axiom, this last fact indicates that there is no condensation above the λ -transition, and that there is condensation below the λ -transition sufficient for the observed flows. It is conventionally understood that the condensation transition is continuous, with condensation increasing from zero at the transition itself. This is evidenced by the continuity in energy, density, and shear viscosity, and it is also predicted by the non-interacting boson model (F. London 1938, Pathria 1972). However it remains to reconcile this conclusion with the discontinuous appearance of superfluidity (flow in thin films and capillaries, and the absence of boiling in the undersaturated liquid) at the transition. In any case, that the condensation is macroscopic is confirmed by the differences on either side of the transition in the behavior of the energy and heat capacity, and also the number (in a given volume), and the flow, since these are all extensive thermodynamic variables.

It has always been assumed, ever since Einstein (1924, 1925) first asserted it, that Bose-Einstein condensation is solely into the ground energy state. However, the experimental fact that there is no latent heat at the λ -transition argues against this since the appearance of a macroscopic number of bosons with zero energy would create a sudden macroscopic change in energy. Rather, the absence of latent heat suggests that the number of bosons in any given energy range is the same before and after condensation. This is consistent with a transition from singly to multiply occupied momentum states, as in the second axiom above, since this can be accomplished in any kinetic energy neighborhood by increasing the momenta of some bosons while decreasing that of others without changing

the total energy.

A caveat to this deduction is that if the amount of macroscopic condensation is zero at the λ -transition, then it might be possible for the condensed bosons to occupy solely the ground energy state without a macroscopic energy discontinuity. However the full weight of evidence is that condensation occurs in multiple low-lying momentum states. For example, for non-interacting (ideal) bosons the occupancy of the ground energy state is an intensive thermodynamic variable (Attard 2025) (this conclusion also holds on general thermodynamic grounds for interacting particles), whereas the experimental evidence is that the λ -transition is a transition in an extensive thermodynamic variable. Also, bosons involved in superfluid flow necessarily have non-zero velocity, which by definition means that they cannot be in the ground energy state.

The λ -transition and superfluidity have been explored at the molecular level within the framework of quantum statistical mechanics (Attard 2018, 2021, 2025a). Detailed mathematical analysis and computer simulations have revealed the role played by interactions between the ^4He atoms, which were missing in earlier modeling with ideal bosons.

There is an important difference between classical statistical mechanics (Attard 2002) and quantum statistical mechanics formulated in classical phase space (Attard 2021) that is directly relevant to Bose-Einstein condensation and the λ -transition. In classical statistical mechanics, the entropy of a macrostate is the logarithm of the weighted sum of the molecular configurations giving that macrostate. This is, in essence, Boltzmann's original explanation of entropy. Hence the partition function, which is essentially the total entropy, is an integral over phase space. In quantum mechanics, the wave function for bosons must be symmetrized by summing over all permutations. Each permutation of a configuration is a new configuration. In quantum statistical mechanics, in addition to the integral over phase space, one also has to sum over all permutations to obtain the total entropy.

In phase space each boson has a position and a momentum, with the latter most usefully quantized in the vicinity of and below the λ -transition. A permutation swaps the momenta of different bosons. Permuting the momenta of condensed bosons all in the same momentum state leaves the configuration unchanged. Such permutations have unit weight, and the occupation entropy, which is the logarithm of the number of these permutations, is what ultimately drives Bose-Einstein condensation.

Using quantum statistical mechanics to explain the λ -transition means identifying both the regions of phase space and the particular types of permutations that dominate. Most permutations give rise to highly oscillatory weights that cancel with small changes in the position or momentum configuration. The dominant permutations give real, positive weights that are insensitive to small changes in configuration. The specific types of permutation that significantly contribute to the total entropy

depend upon the thermodynamic state of the system.

At higher temperatures the number of accessible momentum states far exceeds the number of bosons. In this case every boson is the sole occupant of its own momentum state, and there is no condensation. All permutations give highly oscillatory and therefore canceling weight factors, and so only the identity permutation gives a non-zero phase space weight. This is the classical regime.

The number of accessible momentum states decreases with decreasing temperature. Obviously there comes a temperature when for a fixed number of bosons it is impossible to prevent the multiple occupancy of momentum states. This is the condensed or quantum regime. Approaching the transition to the quantum regime, and deep inside it, there are classes of permutations that give real, positive weights, and these therefore must be taken into account.

On the high temperature side of the λ -transition the divergence of the heat capacity is due to the growth in number and size of position permutation loops. A position loop is a cyclic permutation around a ring of bosons with successive neighbors in close spatial proximity. These loops begin to form when the Gaussian with thermal wavelength width overlaps with the first peak in the pair distribution function: the thermal wavelength increases with decreasing temperature, and the first peak is located at about the diameter of the ^4He atom, and increases in height with decreasing temperature. These position permutation loops are a subset of all the possible permutations: their real positive weight, which is less than unity for each loop, results from averaging over momenta and it is insensitive to small changes in position configuration. The loops arise from wave function symmetrization, which itself sums over all possible permutations of the bosons. The sum of the weights attached to these position permutation loops contributes to the entropy of the system.

As mentioned, permutations amongst condensed bosons all in the same momentum state have unit weight and begin to dominate below the λ -transition. The total number of permutations due to such bosons is just the product of the factorials of the momentum state occupancy, and this also contributes to the entropy of the system. These particular permutations can be constructed from what I call momentum permutation loops, in contrast to position permutation loops. The sum of all momentum loops constructed from bosons in a momentum state is the factorial of the occupancy of that state. In practical terms calculations are performed with occupancies rather than with momentum loops. But in conceptual terms the fact that loops must be disjoint underscores the point that an individual boson cannot belong to both a momentum and a position permutation loop in a single permutation. Whereas position permutation loops are compact and localized at the molecular level in position space, momentum loops are non-localized: bosons in the same momentum state can be permuted

with unit weight even when they are separated by macroscopic distances.

Position and momentum permutation loops are the two most important ways to formulate wave function symmetrization, and they appear sufficient to account for most aspects of the λ -transition and superfluidity. It makes sense therefore in the first instance to factorize the phase space weight that accounts for wave function symmetrization into pure position and momentum loop symmetrization functions. The loops that form any permutation must be disjoint, which is to say that a particular boson can be in only one loop in any given permutation. Therefore, in any configuration only currently condensed bosons contribute to the momentum loop symmetrization function, and only currently uncondensed bosons (and condensed bosons not currently involved in momentum permutation loops) contribute to the position loop symmetrization function. Hence the two types of loops compete for the available bosons and shift the equilibrium between them. Which one dominates depends upon the associated entropy.

This is the simplest binary description: bosons are either condensed or uncondensed, and loops are either pure position or pure momentum. In a more nuanced picture, which is necessary to explain the full range of observed phenomena, it is only a subset of the condensed bosons, namely those in the most highly occupied momentum states, that are entropically favored by permutations within their state at the expense of the entropy lost by destroying the position permutation loops from which they are excluded. Also mixed chains, which are open position loops with a condensed boson at the head and uncondensed bosons forming the tail, appear necessary to account fully for the far side of the λ -transition. These are discussed in more detail below and in the text.

The number and size of position permutation loops with significant weight grow approaching the λ -transition from the high temperature side due to the increase of the thermal wavelength and of the peak of the pair distribution function. At the molecular level position loops are structurally organized in position space. In the binary picture, the transformation of an uncondensed to a condensed boson with momentum loop permutations destroys all the position loops it was part of, and the system loses the associated position loop symmetrization entropy. On the high temperature approach to the λ -transition the available position symmetrization entropy per boson is higher than the available occupation entropy for condensed bosons, which means that position loops suppress condensation in this regime. The computational results below confirm this to be true immediately preceding the λ -transition in the regime where the heat capacity is diverging. This is consistent with the experimental evidence for the absence of superfluidity above the λ -transition, namely that it implies the absence of condensed bosons.

This is an important difference between the ideal and the interacting boson models of the λ -transition. The

ideal boson model has no positional structure or position loops and no physical mechanism to suppress condensation. It is simply asserted in the ideal boson model that the ground state is unoccupied above the transition, and that condensation occurs, and only occurs, when the excited states become full within the ideal boson model (F. London 1938, Pathria 1972). For non-interacting bosons the peak in the heat capacity is finite, $C_V^{\text{id}}/Nk_B = 1.925$ (Attard 2025a, F. London 1938, Pathria 1972). For real ^4He (Lipa *et al.* 1996) and for Lennard-Jones ^4He (Attard 2025a) the peak in the heat capacity is infinite. In the calculations for interacting bosons the divergence of the heat capacity is due to the rapid growth in size and number of position permutation loops.

Indirect experimental evidence for the position loop picture may be seen in the behavior of the density of liquid ^4He on the saturation curve. It is significant that with decreasing temperature the density first increases approaching the λ -transition and then decreases thereafter. Position permutation loops are the part of Bose-Einstein condensation that is linked to the atomic structure of the liquid. For liquid ^4He above the λ -transition, the entropy associated with position permutation loops gives an effective short-ranged attraction to the atoms (the weight of any one position loop increases with decreasing distance between neighbors due to the thermal wavelength Gaussian). The growth in position permutation loops approaching the λ -transition and their decrease after it affects the attractions between the atoms, which is reflected in the behavior of the density.

Further experimental evidence for the existence of position permutation loops may be gleaned from the divergence of the heat capacity on the high-temperature side of the λ -transition. This cannot be due to condensation in low-lying momentum states, since superfluidity is absent above the λ -transition. It is instead due to energy tied up in position permutation loops as these first increase and then decrease in number and size with decreasing temperature.

What causes condensation to finally emerge (or re-emerge) at and below the λ -transition? The experimental observation that the energy and density are continuous through the λ -transition, and that the divergence in the heat capacity is approximately symmetrical on each side of the transition (Lipa *et al.* 1996) says that the position permutation loops begin to decline after the λ -transition, and that they do so in a continuous manner. The computational evidence is that the divergence in the heat capacity is due to the growth in size of position permutation loops. But the fact that mixed position chains have more entropy than pure position loops of the same size means that the mixed chains must re-emerge at the divergent peak of the transition. Hence position permutation loops are increasingly converted into mixed permutation chains on the far side of the λ -transition. These have a condensed boson at the head, and such condensed bosons also participate in pure momentum loops independent of their tail. At the peak of the λ -transition, the large po-

sition permutation loops as well as the tails of the mixed chains block further growth and the system becomes saturated. As the temperature is decreased, the occupation entropy of the condensed bosons increases, which makes it favorable for long chains to be cut into smaller chains, and the relative number of condensed bosons to increase. The increase in condensed bosons in highly occupied low lying momentum states reduces the heat capacity. This description of the far side of the λ -transition is consistent with the number of condensed bosons increasing from zero, and with each one converting the position permutation loops it had been part of to a mixed chain. The close structural relationship between pure position loops and mixed position chains provides a relatively smooth path from the near to the far side of the λ -transition.

Of course it is an overly simplistic consequence of the binary picture of condensation that there is a single occupation entropy applicable to every condensed boson. A more detailed analysis gives a bespoke entropy that depends upon the actual occupation of the momentum state in which the condensed boson currently resides. In this case it is the condensed bosons that are in the most highly occupied momentum states that are the first to be favored by the entropy of internal permutations within their state over that of the position loops that they would otherwise participate in. To see this note that the near side of the λ -transition is dominated by position permutation loops with no condensed bosons, and the far side sees the emergence of mixed chains and condensed bosons. The temperature difference between these two cases is a fraction of a Kelvin. This means that the position loop entropy per boson is almost the same as the mixed chain loop entropy per boson. In these circumstances it is the condensed bosons in the most highly occupied low lying momentum states that first tip the balance. On the far side of the λ -transition the re-emergence of condensed bosons is continuous rather than discontinuous, which is to say that although the number of condensed bosons must be macroscopic (otherwise the temperature gradient of the energy, the density, and the shear viscosity would be unaffected), the fraction of condensed bosons must begin from zero at the λ -transition itself. This more nuanced picture gives a condensation transition that begins with zero fraction of condensed bosons in highly occupied states in a more credible way than the binary all-or-nothing picture.

This can also be reconciled with the apparent discontinuity in superfluidity at the λ -transition by noting that it is these condensed bosons in the most highly occupied momentum states that selectively and most efficiently contribute to superfluid flow in confined geometries. The volume of these flows is generally many times smaller than the volume of the system. Also, the driving forces for these flows probably selects condensed bosons in the most highly occupied momentum states.

It must be emphasized that it is not condensed bosons *per se* that are excluded from position permutation loops and that are responsible for superfluidity. Rather it is

condensed bosons that are participating in permutations within their own momentum state that are excluded, and it is only when the state is highly occupied that exclusion is favorable, and that the viscosity is significantly reduced.

The above discussion of Bose-Einstein condensation and the λ -transition barely touches on the relationship between Bose-Einstein condensation and superfluidity. That is, at the molecular level how is it that condensed bosons give rise to flow without viscosity? Recent analysis and quantum molecular dynamics computer simulations have provided an answer to this important question (Attard 2025b). It turns out that the rate of change of momentum for a condensed boson in response to an applied force is inversely proportional to the occupancy of its momentum state, which for highly occupied states is significantly less than that given by Newton's second law of motion. This effect is due to the internal permutations of the bosons within the momentum state, and only condensed bosons involved in such momentum permutation loops have the reduced rate of change of momentum. Since non-equilibrium thermodynamics shows that the shear viscosity is the time correlation function involving the time rate of change of the first momentum moment (Attard 2012), this explains the reduction or absence of viscosity in superfluid flow. Condensed bosons in more highly occupied momentum states are likely selectively involved in superfluid flow, which explains the efficacy of this mechanism.

This dynamic mechanism is consistent with the competition between position and momentum loops that was discussed above as determining the λ -transition. For a boson in a position loop, the Gaussian thermal wavelength form for the loop bond weight emerges after averaging over the momentum. A condensed boson permuting with others in a highly occupied momentum state spends a larger amount of time with unchanged momentum than an uncondensed boson, or a condensed boson in a few-occupied state. In other words the conditions for the formation of a position loop with real, positive weight occur more frequently for an uncondensed than for a condensed boson.

II. ANALYSIS

A. Condensed and Uncondensed Bosons

I now give some quantitative numerical analysis for interacting bosons that shows the suppression of condensation above the λ -transition. I work mainly with the binary division of condensed and uncondensed bosons.

Consider a subsystem of N interacting bosons in a cubic volume $V = L^3$ able to exchange energy with a reservoir of temperature T . These bosons are divided into disjoint sets of N_0 condensed bosons and N_* uncondensed bosons, with $N = N_0 + N_*$. It would be more accurate to say that the bosons in the set N_* participate in posi-

tion permutation loops, and bosons in the set N_0 participate in momentum permutation loops. The latter do not necessarily belong to highly occupied momentum states, although at low temperatures I expect most to do so. I use N_0 as a constraint with which to minimize the free energy, to which there are four contributions: the analytic quantum free energy for N_0 non-interacting bosons, the analytic classical free energy for N_* non-interacting atoms, the position loop grand potential for N_* interacting bosons, and the classical configurational integral for N interacting atoms.

At high temperatures, there are no position permutation loops, nor are there multiply occupied momentum states. This is the classical regime, and the optimum numbers of the two types of bosons are equal, $\bar{N}_0 = \bar{N}_*$, $T \gg T_\lambda$. In this regime it is a little misleading to call the bosons in the set N_0 ‘condensed’.

I intend to show that the optimum number of condensed bosons just above the λ -transition vanishes, $\bar{N}_0 = 0$. Below the λ -transition temperature I expect condensation, $\bar{N}_0 \gtrsim \bar{N}_*$, but I do not actually show this to be the case. Because the momentum state and the kinetic energy of the condensed bosons is independent of their position, their distribution amongst the momentum states is that of non-interacting bosons. For the appropriate fugacity z , the analytic ideal boson expression for the momentum state occupancy, $\bar{N}_{\mathbf{a}}^{\text{id}}(z)$, satisfies $\sum_{\mathbf{a}} \bar{N}_{\mathbf{a}}^{\text{id}}(z) = N_0$. This same fugacity allows the number of ‘proper’ condensed bosons to be determined, eg. the bosons in multiply occupied momentum states, $\bar{N}_{\mathbf{a}}^{\text{id}}(z) > 1$. It is emphasized that although the momentum distribution amongst the bosons excluded from position permutation loops is ideal, interactions between all bosons are still accounted for in the position configuration integral, as will be seen.

B. Partition Function in Phase Space

The phase space probability density, which was derived in earlier work (Attard 2018, 2021, 2025a Ch. 3), is slightly modified here. Whereas the conventional view of Bose-Einstein condensation holds that condensation is into the ground energy state (Le Bellac *et al.* 2004, F. London 1938, Pathria 1972), the actual evidence is that condensation is into multiple low-lying momentum states (Attard 2025a Chs 2 and 3). Most of the analysis in Ch. 3 of Attard (2025a) was based on the so-called binary division approximation, originally used by F. London (1938), which indeed invokes the ground state as the single state for condensation. The present formulation of the partition function improves upon this by analyzing condensation into multiple momentum states.

The present model uses an augmented phase space that has an additional variable s^N , with $s_j = 0$ if boson j is excluded from position loops and $s_j = 1$ otherwise. It is not necessary to immediately take the continuum

momentum limit, and so initially all bosons have momenta that are integer multiples of $\Delta_p = 2\pi\hbar/L$. This quantization condition arises from the Hermiticity of the momentum operator (Attard 2025b Appendix B). With this additional variable the occupancy of the one-particle momentum state \mathbf{a} is given by

$$N_{\mathbf{a}}(\mathbf{p}^{N_0}) = \sum_{j=1}^N \delta_{s_j,0} \delta_{\mathbf{p}_j, \mathbf{a}} = \sum_{j \in N_0} \delta_{\mathbf{p}_j, \mathbf{a}}, \quad (2.1)$$

where Kronecker- δ s appear.

The formulation of quantum statistical mechanics in classical phase space (Attard 2018, 2021) introduces two functions of phase space, namely the commutation functions, ω , which accounts for the non-commutativity of the position and momentum operators, and the symmetrization function, η , which accounts for wave function symmetrization.

Bose-Einstein condensation is a non-local phenomenon that is dominated by bosons beyond the range of the pair potential (Attard 2025a Chs. 2 and 3). Since the commutation function is a short-ranged function, decaying asymptotically as the gradient of the pair potential, the commutation function is neglected here.

The symmetrization function is the sum over all permutations of the ratio of the original and the permuted momentum eigenfunction. The terms in the sum lie on the unit circle in the complex plane and mostly cancel due to rapid oscillation with small changes in position or momentum. The two types of permutations that survive are those between bosons in the same momentum state, and those between neighboring bosons in position space that form a so-called position permutation loop. I make the approximation that the symmetrization function can be written as the product of pure permutations of each type

$$\eta(\mathbf{q}^N, \mathbf{p}^N) = \eta_*(\mathbf{q}^{N_*}, \mathbf{p}^{N_*}) \eta_0(\mathbf{p}^{N_0}). \quad (2.2)$$

By definition an individual boson cannot participate in more than one permutation loop at a time (Attard 2018, 2021). Hence for this factorization to be valid the two symmetrization functions have to be based upon disjoint sets. Specifically, a condensed boson that contributes to the momentum permutation loops embodied in η_0 cannot contribute to the position permutation loops in η_* .

The symmetrization function for the condensed bosons depends only upon their momentum configuration,

$$\eta_0(\mathbf{p}^{N_0}) = \prod_{\mathbf{a}} N_{\mathbf{a}}!. \quad (2.3)$$

This is the total number of ways of permuting condensed bosons within the same momentum states. It is the permutations of the condensed bosons that give rise to the occupation entropy that ultimately drives Bose-Einstein condensation and superfluidity. In previous work (Attard 2025a Eq. (3.3)), the binary division approximation considered condensed bosons to be those in the momentum

ground state. It also denoted them with a subscript 0, so that $\mathbf{p}_j = \mathbf{0}$, $j \in N_0$, and $\eta_0(\mathbf{p}^{N_0}) = N_0!$. In contrast, the present analysis eshews condensation solely into the ground state.

The symmetrization function for position permutation loops, η_* , excludes condensed bosons, $N_* = N - N_0$. As just mentioned, because any one boson can be in only one permutation loop at a time, the factorization of the symmetrization function can only be valid when the two factors are based on disjoint sets of bosons. Because the spacing between momentum states goes to zero in the thermodynamic limit, the momentum quadrature can be performed (Attard 2018, 2021),

$$\begin{aligned} \eta_*(\mathbf{q}^{N_*}, \mathbf{p}^{N_*}) &\Rightarrow \bar{\eta}_*(\mathbf{q}^{N_*}) \\ &= \prod_{l=2}^{l_{\max}} e^{G^{(l)}(\mathbf{q}^{N_*})}. \end{aligned} \quad (2.4)$$

This is a mean field approximation, where the position permutation loop symmetrization function for the current configuration in phase space is replaced by its momentum average, $\bar{\eta}_*(\mathbf{q}^{N_*})$. This momentum-averaged position loop symmetrization function is real and non-negative. The total of the l -loop Gaussians is

$$G^{(l)}(\mathbf{q}^{N_*}) = \sum_{j_1, \dots, j_l}^{N_*} G^{(l)}(\mathbf{q}_{j_1}, \dots, \mathbf{q}_{j_l}), \quad (2.5)$$

where the prime on the summation indicates that all indeces must be different and that only distinct loops are counted. An individual l -loop Gaussian is

$$G^{(l)}(\mathbf{q}_{j_1}, \dots, \mathbf{q}_{j_l}) = \prod_{k=1}^l e^{-\pi q_{j_k, j_{k+1}}^2 / \Lambda^2}, \quad j_{l+1} \equiv j_1. \quad (2.6)$$

The thermal wave length is $\Lambda \equiv \sqrt{2\pi\hbar^2\beta/m}$.

With these the phase space weight is (Attard 2025a Eq.(3.61))

$$\begin{aligned} w(\mathbf{p}^N, \mathbf{q}^N, s^N | N, V, T) \\ = \frac{1}{N!V^N} e^{-\beta\mathcal{K}(\mathbf{p}^N)} e^{-\beta U(\mathbf{q}^N)} \eta_0(\mathbf{p}^{N_0}) \bar{\eta}_*(\mathbf{q}^{N_*}). \end{aligned} \quad (2.7)$$

Here \mathcal{K} is the kinetic energy, U is the potential energy, and $\beta \equiv 1/k_B T$. The momenta \mathbf{p}^N are discrete with spacing Δ_p . Below I often use $\{\mathbf{q}, \mathbf{p}\}$ as short-hand for $\{\mathbf{q}^N, \mathbf{p}^N\}$.

At high temperatures, where both the occupancy entropy, $S^{\text{occ}} = k_B \ln \eta_0$, and the position permutation entropy, $S_* = k_B \ln \bar{\eta}_*$, are zero, there is nothing to distinguish $s_j = 0$ and $s_j = 1$; both occur with equal probability. In this case any boson with $s_j = 0$ is likely to be the sole occupant of its momentum state, and it does not behave as condensed bosons behave. This changes at lower temperatures where, due to condensed bosons being excluded from position permutation loops, there

is a competition between the occupation entropy of condensed bosons, and the position permutation entropy of uncondensed bosons.

The grand partition function is (cf. Attard 2025a Eq. (3.1))

$$\begin{aligned} \Xi^+(z, V, T) \\ = \sum_{N=0}^{\infty} \frac{z^N}{V^N N!} \sum_{\mathbf{p}} \int d\mathbf{q} e^{-\beta\mathcal{H}(\mathbf{q}, \mathbf{p})} \eta_*(\mathbf{q}, \mathbf{p}) \omega(\mathbf{q}, \mathbf{p}) \\ \approx \sum_{N=0}^{\infty} \sum_{\mathbf{s}=0,1} \frac{z^N}{V^N N!} \\ \times \sum_{\mathbf{p}} \int d\mathbf{q} e^{-\beta\mathcal{H}(\mathbf{q}, \mathbf{p})} \bar{\eta}_*(\mathbf{q}^{N_*}) \eta_0(\mathbf{p}^{N_0}) \\ = \sum_{N_0=0}^{\infty} \sum_{N_*=0}^{\infty} \frac{z^N}{V^N N!} \frac{N!}{N_0! N_*!} \\ \times \sum_{\mathbf{p}} \int d\mathbf{q} e^{-\beta\mathcal{H}(\mathbf{q}, \mathbf{p})} \bar{\eta}_*(\mathbf{q}^{N_*}) \eta_0(\mathbf{p}^{N_0}), \end{aligned} \quad (2.8)$$

where the classical Hamiltonian is $\mathcal{H} = \mathcal{K} + U$. The binomial coefficient is the number of ways of assigning labels to the N_0 and N_* condensed and uncondensed bosons; it is the weight required for the specific boson assignment implicit once the sum over \mathbf{s} has been replaced by the sums over number. This result for the grand partition function is equivalent to Attard (2025a Eq. (3.3)), except that the condensed bosons are here not confined to the momentum ground state.

The momentum part of the grand potential for condensed bosons is just ideal. The corresponding grand potential is given by

$$\begin{aligned} e^{-\beta\Omega_0^{\text{id}}} &\equiv \sum_{N_0=0}^{\infty} \frac{z^{N_0}}{N_0!} \sum_{\mathbf{p}^{N_0}} e^{-\beta\mathcal{K}(\mathbf{p}^{N_0})} \eta_0(\mathbf{p}^{N_0}) \\ &= \sum_{N_0=0}^{\infty} \frac{z^{N_0}}{N_0!} \sum_{\mathbf{p}^{N_0}} e^{-\beta\mathcal{K}(\mathbf{p}^{N_0})} \prod_{\mathbf{a}} N_{\mathbf{a}}! \\ &= \prod_{\mathbf{a}} \sum_{N_{\mathbf{a}}=0}^{\infty} z^{N_{\mathbf{a}}} e^{-\beta N_{\mathbf{a}} a^2 / 2m} \\ &= \prod_{\mathbf{a}} [1 - z e^{-\beta a^2 / 2m}]^{-1}. \end{aligned} \quad (2.9)$$

The average number of condensed bosons is

$$\begin{aligned} \bar{N}_0(z) &= \frac{z \partial(-\beta\Omega_0^{\text{id}})}{\partial z} \\ &= \sum_{\mathbf{a}} \frac{z e^{-\beta a^2 / 2m}}{1 - z e^{-\beta a^2 / 2m}} \\ &\equiv \sum_{\mathbf{a}} \bar{N}_{\mathbf{a}}. \end{aligned} \quad (2.10)$$

For a given (constrained) number of condensed bosons, this determines the fugacity $z = \bar{z}(N_0)$ implicitly as the one that satisfies $\bar{N}_0(z) = N_0$.

The ideal Helmholtz free energy for the condensed bosons is $F_0^{\text{id}}(N_0, V, T) = \Omega_0^{\text{id}}(\bar{z}, V, T) + \bar{\mu}N_0$, with $z = e^{\beta\mu}$. Its number derivative is (Attard 2002 Ch. 3)

$$\frac{\partial F_0^{\text{id}}(N_0, V, T)}{\partial N_0} = \bar{\mu}(N_0, V, T). \quad (2.11)$$

The number of proper condensed bosons (ie. those in multiply occupied momentum states) for a given number of condensed bosons could be taken to be

$$\bar{N}_{00}(N_0) = \sum_{\mathbf{a}} \bar{N}_{\mathbf{a}} \Theta(\bar{N}_{\mathbf{a}} - 1). \quad (2.12)$$

Here the unit Heaviside step function appears, and $z = \bar{z}(N_0)$. Obviously $\bar{N}_{\mathbf{a}}(z, V, T)$ is the average occupancy of the momentum state \mathbf{a} for the current number of condensed bosons N_0 . This somewhat arbitrarily sets an occupancy of unity as the beginning of proper condensation; a larger value would likely be more useful.

A variational procedure to determine the number of condensed bosons is required. The constrained free energy can be written as (cf. Attard 2002 Ch. 3)

$$\Omega(N_0|z, N, V, T) = F(N_0, N_*, V, T) + [N_0 + N_*]\mu. \quad (2.13)$$

Since $N_0 + N_* = N$ is held constant, the final term can be neglected. That is, the Helmholtz free energy $F(N_0, N_*, V, T)$ must be minimized with respect to N_0 at constant N .

Using the above expression for the ideal Helmholtz free energy, the Helmholtz free energy for the interacting bosons is given by

$$\begin{aligned} & e^{-\beta F(N_0, N_*, V, T)} \\ &= \frac{1}{V^N N_0! N_*!} \sum_{\mathbf{p}} \int d\mathbf{q} e^{-\beta \mathcal{H}(\mathbf{q}, \mathbf{p})} \bar{\eta}_*(\mathbf{q}^{N_*}) \eta_0 \mathbf{p}^{N_0} \\ &= \frac{e^{-\beta F_0^{\text{id}}(N_0, V, T)}}{V^N \Lambda^{3N_*} N_*!} \int d\mathbf{q}^N e^{-\beta U(\mathbf{q}^N)} \bar{\eta}_*(\mathbf{q}^{N_*}). \end{aligned} \quad (2.14)$$

In the final equality the sum over the momenta of the continuum bosons has been carried out by integration. The difference between this and Attard (2025a §3.1) is the F_0^{id} .

Attard (2025a Eq. (3.8)) developed a loop expansion for the grand potential based on

$$\langle \eta_* \rangle_{\text{cl}} = e^{\langle \bar{\eta}_* \rangle_{\text{cl}}}. \quad (2.15)$$

This is a classical average. The exponent is the sum of single position loops. This expression is valid for large systems in the dilute compact position loop regime. When the loops become large, this expression improperly counts forbidden products of intersecting loops in a way that is not negligible even in the thermodynamic limit.

The present monomer grand potential becomes (cf. Attard 2025a Eq. (3.11))

$$e^{-\beta \Omega^{(1)}(z, V, T)} = \sum_{N_0, N_*} \frac{z^N e^{-\beta F_0^{\text{id}}(N_0, V, T)}}{N_*! \Lambda^{3N_*} V^{N_0}} Q(N, V, T), \quad (2.16)$$

where the position configuration integral is

$$Q(N, V, T) = \int d\mathbf{q}^N e^{-\beta U(\mathbf{q}^N)}. \quad (2.17)$$

The exponential form gives rise to the l -loop grand potential,

$$-\beta \Omega_*^{(l)} = \frac{(N_*)^l}{N^{l-1}} g^{(l)}, \quad g^{(l)} \equiv \frac{1}{N} \langle G^{(l)}(\mathbf{q}^N) \rangle_{N, V, T}^{\text{cl}}. \quad (2.18)$$

The average of the loop Gaussian is calculated in a classical system of N particles, so that $g^{(l)}$ does not depend upon N_0 . It is intensive. The prefactor represents the probability that l bosons chosen randomly for each loop in the original system of N_0 condensed and N_* uncondensed bosons are all uncondensed.

The constrained free energy is therefore taken to be

$$F(N_0|N, V, T) \equiv F(N_0, N, V, T) \quad (2.19)$$

$$\begin{aligned} &= F_0^{\text{id}}(N_0, V, T) + k_B T \ln[N_*! \Lambda^{3N_*} V^{N_0}] \\ &\quad - k_B T \ln Q(N, V, T) - k_B T \sum_{l=2}^{l_{\text{max}}} \frac{(N_*)^l}{N^{l-1}} g^{(l)}. \end{aligned}$$

The derivative at constant N is

$$\begin{aligned} & \frac{\partial F(N_0|N, V, T)}{\partial N_0} \\ &= \bar{\mu} - k_B T \ln \frac{N_* \Lambda^3}{V} + k_B T \sum_{l=2}^{l_{\text{max}}} l \left(\frac{N_*}{N} \right)^{l-1} g^{(l)}. \end{aligned} \quad (2.20)$$

The fugacity $z = e^{\beta\mu}$ depends on the number of condensed bosons via the ideal boson expression. For a stable minimum in the constrained Helmholtz free energy, the derivative passes from negative to positive with increasing N_0 . The condensed bosons, N_0 , and the uncondensed bosons, $N_* = N - N_0$, are counted once each in the quantum and classical ideal terms. The condensed bosons are excluded from the position permutation loops.

At high temperatures, $z \rightarrow 0$ and $\mu \rightarrow -\infty$. Also $g^{(l)} \rightarrow 0$ as $\Lambda \rightarrow 0$. Note that at high temperatures there is no distinction between condensed and uncondensed bosons, and $\langle s_j \rangle = 1/2$. The quantum ideal fugacity is expected to go over to the classical ideal fugacity, $z^{\text{qu,id}}(N_0) \rightarrow z^{\text{cl,id}}(N_0) = N_0 \Lambda^3 / V$. Since the loop terms are zero at high temperatures, the constrained free energy is a minimum when the first two terms cancel, which occurs when $\bar{N}_0 = \bar{N}_* = N/2$. This is the expected result.

C. Alternative Constrained Free Energy

The preceding analysis is a little unrealistic at higher temperature since in this regime there is no real distinction between ‘condensed’ bosons, $s_j = 0$, and uncondensed bosons, $s_j = 1$, other than the rule that the former are excluded from position permutation loops and

also that they be analyzed with quantum rather than classical formulae. It is dissonant to say that condensed bosons are responsible for superfluidity, when, according to this definition, they comprise 50% of the system at higher temperatures where there is no superfluidity.

An alternative approach is to focus on the lowest momentum states, \mathbf{a} , whose kinetic energy is small compared to the thermal energy, $\beta a^2/2m \ll 1$. These are the states that are most likely multiply occupied and therefore they fit better the definition of condensed. We can use the total number of bosons in these states, which we denote N'_0 , as the constraint. Whereas the occupancy of the ground state is an intensive variable, the number of bosons in states with negligible kinetic energy, the present N'_0 , is an extensive variable and it is therefore macroscopic (Attard 2025a §2.5).

The constrained Helmholtz free energy (after integrating over the remaining momenta) is

$$\begin{aligned} \beta F(N'_0|N, V, T) &= \ln[N_*! \Lambda^{3N_*} V^{N'_0}] \\ &\quad - \ln Q(N, V, T) - \sum_{l=2}^{l_{\max}} \frac{N_*^l}{N^{l-1}} g^{(l)}. \end{aligned} \quad (2.21)$$

where $N_* = N - N'_0$ is the number of uncondensed bosons. As above, the occupation entropy, $\eta_0 = \prod_{\mathbf{a}} N_{\mathbf{a}}! / N'_0!$, cancels in transforming to the occupation picture for the condensed bosons. There is no kinetic energy contribution because it is negligible compared to the thermal energy for all the condensed bosons. There is no sum over momentum states for the condensed bosons because their occupancies are specified in the constraint N'_0 (but see below). The derivative at constant N is

$$\begin{aligned} \left(\frac{\partial \beta F(N'_0|N, V, T)}{\partial N'_0} \right)_N \\ = -\ln \frac{N_* \Lambda^3}{V} + \sum_{l=2}^{l_{\max}} l \left(\frac{N_*}{N} \right)^{l-1} g^{(l)}. \end{aligned} \quad (2.22)$$

This passes from negative to positive with increasing N'_0 at a stable minimum in the free energy.

The ideal contribution from the condensed bosons has been neglected in these. If the N'_0 condensed bosons occupy M_0 low lying momentum states, then the extra contribution to the constrained Helmholtz free energy βF would be $-M_0 \ln[1 + N'_0/M_0]$, with derivative at constant occupancy being $-(M_0/N'_0) \ln[1 + N'_0/M_0]$. This is negligible for large occupancies, which is the definition of a condensed boson.

D. Mixed Loops

The preceding two subsections were based on pure loops, namely position loops composed solely of uncondensed bosons, and momentum loops giving permutations between condensed bosons all in the same momentum state. The product of the respective symmetrization

functions was invoked with the justification that since the two sets of bosons were disjoint, the pure loops could be multiplied without violating the condition that a boson could belong to only one loop at a time.

However the exponential ansatz that gives rise to the loop grand potential for the position permutation loops already fails to enforce strictly this condition since it implicitly allows the product of position loops containing the same uncondensed boson. It is believed that such overlaps are negligible in the thermodynamic limit, although this is likely to be only the case in the dilute compact loop regime.

This is one reason to consider mixed position permutation loops containing condensed and uncondensed bosons. A second reason is that there appears to be missing from the above analysis any physical mechanism to drive the re-emergence of condensed bosons on the far side of the λ -transition. This might be called the Lazarus transition, because the condensed bosons that were dead on the near side suddenly spring back to life at the peak of the λ -transition.

It is fairly clear that condensed bosons excluded from position loops composed purely of uncondensed bosons block and disrupt such loops. This leads to the suppression of condensation during the growth of position loops on the near side of the λ -transition. But beyond the general increase in occupancy of low-lying momentum states with decreasing temperature there is nothing in the pure loop analysis that specifically drives condensation once position permutation loops have begun to form. It is arguable that mixed loops would provide such a mechanism since they directly link condensed bosons to the growing loops of which they are part.

Attard (2025a §3.2) previously analyzed mixed loops. Much of that analysis is reproduced here but there is one significant difference. Attard (2025a §3.2) argued that it was necessary to respect the orthogonality of momentum eigenfunctions by subtracting the disconnected contributions to the averages of the mixed loops, so that the multi-particle density was replaced by the total correlation function, giving so-called corrected (or connected) averages. The current judgement of the author is that such arguments are spurious, and in what follows the ordinary average using the usual (disconnected) multi-particle density is invoked.

Attard (2025a §3.2.3) analyzed dressed condensed bosons based upon an l -chain, which has $l - 1$ uncondensed bosons forming the tail, and a condensed boson, labeled j_l , forming the head. The condensed bosons are defined as in the preceding subsection, namely there are N'_0 of them, each in a low-lying momentum state, $\mathbf{p}_{j_l} \approx \mathbf{0}$. For this reason chains are localized but form an open loop, $q_{j_1, j_l} \gg \Lambda$. Non-local loops of chains may be formed head-to-tail. There are $N'_0!$ ways of forming products and concatenations of these chains. This assumes that they have no uncondensed bosons in common, which will be valid in the dilute condensation, small chain regime.

The l -chain Gaussian for an individual condensed boson j is (cf. Attard 2025a Eq. (3.36))

$$\tilde{g}_j^{(l)}(\mathbf{q}_j; \mathbf{q}^{N_*}) = \sum_{j_1, \dots, j_{l-1}}^N \prod_{k=1}^{l-1} e^{-\pi q_{j_k, j_{k+1}}^2 / \Lambda^2}, \quad j_l \equiv j, \quad (2.23)$$

and $\tilde{g}_j(\mathbf{q}_j; \mathbf{q}^{N_*}) = \sum_{l=2}^{l_{\max}} \tilde{g}_j^{(l)}(\mathbf{q}_j; \mathbf{q}^{N_*})$. This can be justified by averaging the uncondensed bosons' momenta over a contour in the complex plane, together with the fact that the head boson is in a low-lying momentum state, $\mathbf{p}_{j_l} \approx \mathbf{0}$.

Actually, just as for loops, it is not necessary to distinguish condensed and uncondensed bosons as the classical average in an N, V, T system will soon be taken. What distinguishes a chain from a loop is that there is no q_{j_l, j_1} bond. Whereas loops are closed, chains are open, they are satisfied by many more position configurations, and they have greater weight, particularly so as l increases.

The symmetrization function is taken to be the product of pure loops and mixed chains,

$$\begin{aligned} \eta(\mathbf{p}, \mathbf{q}) &= \eta_*(\mathbf{q}^{N_*}) \eta_0(\mathbf{p}^{N'_0}) \prod_{j \in N'_0} [1 + \tilde{g}_j(\mathbf{q}_j; \mathbf{q}^{N_*})] \\ &\Rightarrow \eta_*(\mathbf{q}^{N_*}) N'_0! [1 + \tilde{g}]^{N'_0}. \end{aligned} \quad (2.24)$$

The term unity represents the monomer when the condensed boson is not part of any mixed chain. This is a mean field approximation with \tilde{g} (no argument) being the classical average of the intensive chain Gaussian (see next).

The mixed l -chains require the Gaussian

$$\tilde{G}^{(l)}(\mathbf{q}^N) = \sum_{j_1, \dots, j_l}^N \prod_{k=1}^{l-1} e^{-\pi q_{j_k, j_{k+1}}^2 / \Lambda^2}. \quad (2.25)$$

From this comes the intensive form based on the classical average, which is independent of the division into condensed and uncondensed bosons,

$$\tilde{g}^{(l)} \equiv \frac{1}{N} \langle \tilde{G}^{(l)}(\mathbf{q}^N) \rangle_{N, V, T}^{\text{cl}}. \quad (2.26)$$

Unlike Attard (2025a §3.2.3), it is an ordinary classical average that appears here. Finally, the sum total of loop Gaussians that does depend on the number of condensed bosons is

$$\tilde{g} \equiv \sum_{l=2}^{l_{\max}} \frac{N'_0 N_*^{l-1}}{N^l} \tilde{g}^{(l)}. \quad (2.27)$$

The chain weight \tilde{g} is intensive. The prefactor for the l -loop Gaussian is the probability that of l bosons randomly chosen to form a chain, the head is a condensed boson and the tail is composed of uncondensed bosons, of which there are $N_* = N - N'_0$.

The weight of mixed loops is defined on average rather than for a configuration in phase space. Multiplying the

average chain weights is valid in the small dilute loop regime. The intensive Gaussian chain weight, $1 + \tilde{g}$, is like an extra fugacity for condensed bosons. This result for the symmetrization function links the growth of position loops to condensation, which links superfluidity to the λ -transition. It also suggests the mechanism by which the suppression of condensation on the near side of the λ -transition is overcome.

The constrained Helmholtz free energy (after integrating over the remaining momenta) is

$$\begin{aligned} \beta F(N'_0 | N, V, T) &= \ln[N_*! \Lambda^{3N_*} V^{N'_0}] - \ln Q(N, V, T) \\ &\quad - N'_0 \ln[1 + \tilde{g}] - \sum_{l=2}^{l_{\max}} \frac{N_*^l}{N^{l-1}} g^{(l)}, \end{aligned} \quad (2.28)$$

with $N = N'_0 + N_*$. As in the preceding subsection, we have neglected the ideal contribution from the condensed bosons.

The main difference between the loop and chain contributions is the factor of N'_0 in the series for \tilde{g} . Whereas increasing N'_0 only increases the loop free energy (because it decreases N_*), it can decrease the chain free energy because of the part proportional to N'_0 . One can see that if the fraction of condensed bosons is small and the fraction of uncondensed bosons is large, and $\tilde{g}^{(l)}$ is constant or increasing with l , then the sum over chains will be dominated by large chains, and in fact the chain free energy will be reduced by increasing the fraction of condensed bosons. This is exactly what is required to bring back condensation at and below the λ -transition.

The derivative at constant N is

$$\begin{aligned} &\left(\frac{\partial \beta F(N'_0 | N, V, T)}{\partial N'_0} \right)_N \\ &= -\ln \frac{N_* \Lambda^3}{V} + \sum_{l=2}^{l_{\max}} l \left(\frac{N_*}{N} \right)^{l-1} g^{(l)} \\ &\quad - \frac{\tilde{g}}{1 + \tilde{g}} - \ln[1 + \tilde{g}] \\ &\quad + \frac{1}{1 + \tilde{g}} \left(\frac{N'_0}{N} \right)^2 \sum_{l=2}^{l_{\max}} (l-1) \left(\frac{N_*}{N} \right)^{l-2} \tilde{g}^{(l)}. \end{aligned} \quad (2.29)$$

For small N'_0/N , the first two chain terms, which are linear in N'_0/N , dominate the chain series with the quadratic prefactor. Since $\tilde{g} > 0$ these give a negative force that drives an increase in the number of condensed bosons, as was discussed above.

III. RESULTS

The Monte Carlo algorithm used to simulate Lennard-Jones ^4He and to obtain the loop Gaussians and the heat capacity has been described elsewhere (Attard 2021 §5.4.2). Briefly, the Lennard-Jones pair potential is

TABLE I: Loop Gaussians for saturated Lennard-Jones ^4He . From classical Monte Carlo simulations with loop pruning algorithm with the statistical error being on the order of 0.1% (Attard 2021).

T^*	ρ^*	Λ/σ	$g^{(2)}$	$g^{(3)}$	$g^{(4)}$	$g^{(5)}$
0.35 ^a	1.0214	1.8051	0.559	0.827	1.57	3.97
0.40 ^a	1.0190	1.6886	0.385	0.425	0.611	1.17
0.45 ^a	1.0117	1.5920	0.265	0.223	0.246	0.366
0.50 ^a	0.9433	1.5103	0.167	0.0963	0.0750	0.0763
0.55 ^a	0.9049	1.4400	0.115	0.0505	0.0306	0.0242
0.50 ^b	0.9331	1.5103	0.177	0.105	0.0869	0.0886
0.55 ^b	0.9049	1.4400	0.119	0.0526	0.0333	0.0260
0.60 ^b	0.8872	1.3787	0.0820	0.0278	0.0137	0.00854
0.65 ^b	0.8678	1.3246	0.0565	0.0146	0.00570	0.00277
0.70 ^b	0.8470	1.2764	0.0389	0.00768	0.00236	0.1911
0.75 ^b	0.8282	1.2331	2.70E-02	4.08E-03	9.99E-04	3.03E-04
0.80 ^b	0.8023	1.1940	1.84E-02	2.12E-03	4.06E-04	9.86E-05
0.90 ^b	0.7503	1.1257	8.68E-03	5.71E-04	6.77E-05	1.02E-05
1.00 ^b	0.7009	1.0679	4.17E-03	1.59E-04	1.18E-05	1.16E-06

^aDroplet ^bHomogeneous

$u(r) = 4\epsilon[(\sigma/r)^{12} - (\sigma/r)^6]$. For ^4He , the accepted Lennard-Jones parameters are $\epsilon_{\text{He}} = 10.22k_{\text{B}}\text{J}$ and $\sigma_{\text{He}} = 0.2556\text{ nm}$ (van Sciver 2012). Using instead $\epsilon = 4.8k_{\text{B}}\text{J}$ and $\sigma = 0.36\text{ nm}$ would bring the following results into line with the measured values for the λ -transition temperature and for the saturated liquid density. The Lennard-Jones pair potential was set to zero beyond $R_{\text{cut}} = 3.5\sigma$, and periodic boundary conditions and the nearest neighbor convention were used. The number of atoms in the simulations was $N = 5,000$.

The Lennard-Jones ^4He liquid saturation density at each temperature was obtained from classical simulations of a liquid drop in the center of the system in equilibrium with its own vapor. Results for the heat capacity etc. taken over the central region of this inhomogeneous system were in reasonable agreement with those obtained in a separate simulation of a homogeneous system at the liquid density. The Lennard-Jones ^4He liquid saturation density is about double the measured liquid saturation density of ^4He when using the standard value of σ_{He} . This is due to the approximate nature of the Lennard-Jones pair potential, the neglect of many body potentials, the leading one of which is the Axilrod-Teller triple dipole potential, which is short-ranged and mainly repulsive, and the neglect of the commutation function, which is also short-ranged and predominantly repulsive (Attard 2018, 2021). Increasing σ_{He} by about a factor of 1.4 compensates for the neglect of these repulsive contributions and increases the simulated saturation density to the measured value in SI units. It was judged best to perform the simulations using the Lennard-Jones ^4He liquid saturation density.

Table I shows the loop Gaussians up to $l_{\text{max}} = 5$ obtained on the Lennard-Jones saturated liquid density

TABLE II: Chain Gaussians for saturated Lennard-Jones ^4He .

$k_{\text{B}}T/\epsilon_{\text{He}}$	$\rho\sigma_{\text{He}}^3$	$\tilde{g}^{(2)}$	$\tilde{g}^{(3)}$	$\tilde{g}^{(4)}$	$\tilde{g}^{(5)}$
0.35 ^a	1.0214	2.37E+00	7.55E+00	2.55E+01	9.47E+01
0.40 ^a	1.0190	1.84E+00	4.52E+00	1.18E+01	3.43E+01
0.45 ^a	1.0117	1.45E+00	2.79E+00	5.73E+00	1.35E+01
0.50 ^a	0.9433	1.07E+00	1.51E+00	2.23E+00	3.67E+00
0.55 ^a	0.9049	8.55E-01	9.50E-01	1.11E+00	1.44E+00
0.50 ^b	0.9331	1.13E+00	1.65E+00	2.60E+00	4.27E+00
0.55 ^b	0.9049	8.80E-01	1.00E+00	1.23E+00	1.58E+00
0.60 ^b	0.8872	7.01E-01	6.36E-01	6.19E-01	6.33E-01
0.65 ^b	0.8678	5.60E-01	4.04E-01	3.12E-01	2.55E-01
0.70 ^b	0.8470	4.47E-01	2.57E-01	1.58E-01	1.04E-01
0.75 ^b	0.8282	3.59E-01	1.65E-01	8.13E-02	4.20E-02
0.80 ^b	0.8023	2.85E-01	1.04E-01	4.05E-02	1.67E-02
0.90 ^b	0.7503	1.80E-01	4.10E-02	1.01E-02	2.62E-03
1.00 ^b	0.7009	1.14E-01	1.65E-02	2.58E-03	4.37E-04

^aDroplet ^bHomogeneous

curve. In general the loop Gaussians decrease with increasing temperature. At higher temperatures they decrease with increasing loop size, but at the lowest temperatures shown they appear to form a divergent series. It can be seen that there is good agreement between the results obtained from the simulation of a droplet and those from the homogeneous simulation at the two overlapping temperatures.

Table II shows the chain Gaussians, Eq. (2.26). The statistical error is on the order of 0.1%. As for the loop Gaussians, these decrease with increasing temperature. They also decrease with increasing size except at the lowest temperatures. In general the weight of a given chain is larger than that of the corresponding loop.

At the lowest temperatures results for the free energy for a finite number of loop Gaussians should be treated cautiously. That $g^{(l)}$ or $\tilde{g}^{(l)}$ are flat or increasing with l indicates that large loops are favored. In the large loop regime the exponential form for the position permutation loop symmetrization function is likely to fail because of loop intersections. Basically when the product of a few loops are involved, the intersections are negligible in the thermodynamic limit. But not so for many products. When the $g^{(l)}$ and $\tilde{g}^{(l)}$ are less than unity, then only terms with few products contribute to the series expansion that gives the exponential. When the loop or chain Gaussians are larger than unity, then individual terms comprise so many products that intersections are no longer negligible, even in the thermodynamic limit. For loops, the case $T^* = 0.50$ is probably just acceptable, and for chains $T^* = 0.60$ is probably almost acceptable.

Figure 1 shows the most likely number of atoms that are excluded from the position permutation loops along the Lennard-Jones saturation curve. This was obtained by minimizing the free energy, Eq. (2.19), using the pure position loop Gaussians in Table I. At high temperatures $\bar{N}_0 = N/2$, as expected. This says that there is no differ-

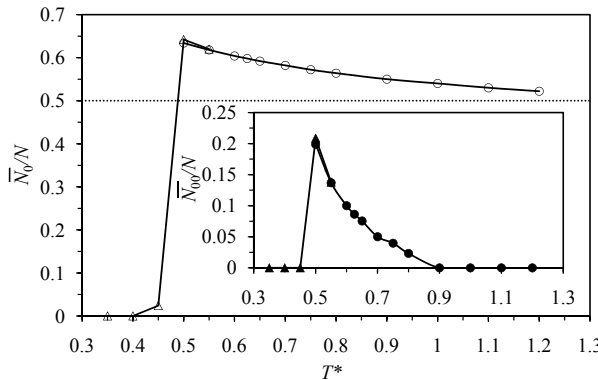


FIG. 1: Most likely fraction of excluded Lennard-Jones ^4He atoms, Eq. (2.19). The circles are from homogeneous simulations and the triangles from simulations of a droplet. The dotted line and the lines connecting symbols are eye guides. **Inset.** The most likely fraction of Lennard-Jones ^4He atoms in momentum states with $\bar{N}_a > 1$.

ence between the classical and quantum formulations in this regime. As the temperature is decreased, the fraction of quantized (excluded) bosons rises above 50%. This says that the contribution from the occupation entropy increases faster than that of position loops, so that it is favorable to use the quantum form for the ideal contribution, which implicitly includes the occupation entropy, to the free energy rather than the classical ideal form. In the high temperature regime, $T^* \gtrsim 0.5$, the thermal wavelength is not much bigger than the atomic diameter, $\Lambda < 1.5\sigma$, and so there are likely to be many atoms that are not close to any neighbor, $q_{j_k, j_{k+1}} \gtrsim \sigma$, which means that they are not part of loops with significant weight. (Recall that the bond weight is $e^{-\pi q_{j_k, j_{k+1}}^2 / \Lambda^2}$.) These monomers can become condensed bosons without losing any position permutation loop entropy.

At $k_B T / \varepsilon_{\text{He}} = 0.45$ a sharp transition takes place to a regime in which all bosons are included in the position permutation loops and there are no condensed bosons. Presumably here almost all atoms have neighbors within the thermal wavelength and can form position permutation loops. Evidently the entropy to be gained from the multiple occupancy of states is less than that lost by disrupting position permutation loops. The requirement for such a transition to enable consistency with experimental observation was discussed at length in the introduction.

It should be emphasized that at $k_B T / \varepsilon_{\text{He}} = 0.45$ the Gaussian loop series is borderline convergent, if not actually divergent. This means that we are likely in the regime where large loops form. In this regime the exponential form for the pure position loop symmetrization function may not be accurate because the contribution from forbidden intersecting loops (ie. loops with a boson or bosons in common) is not negligible in the thermodynamic limit. If the exponential form is not reliable then the constrained free energy will be quantitatively inaccurate. It is probably not a coincidence that the pre-

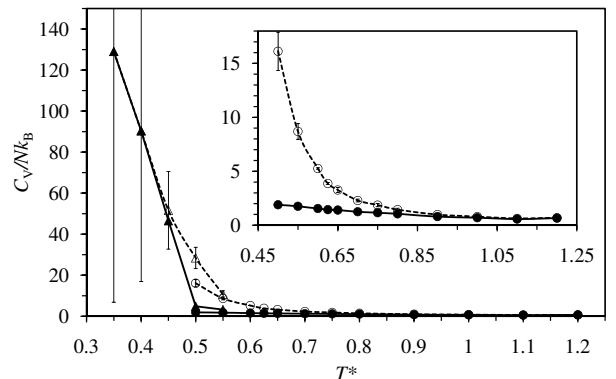


FIG. 2: The specific heat capacity of Lennard-Jones ^4He . The circles are from homogeneous simulations and the triangles from simulations of a droplet. Using Eq. (2.19), the solid symbols have \bar{N}_0 atoms excluded from the position permutation loops, whereas the open symbols have all atoms included in the loops. The lines connecting symbols are eye guides. The error bars give the 95% confidence level. **Inset.** Magnification at higher temperatures.

dicted suppression of condensation occurs just as large loops become common.

What is perhaps a little surprising in Fig. 1 are the results at higher temperatures, namely the increase in excluded bosons from 50% prior to the suppression transition. One might wonder that perhaps this suggests the existence of superfluidity prior to the λ -transition. However the inset to the figure makes it clear that only a relatively small fraction of bosons are in states with an average ideal occupancy greater than unity. Recall that condensed bosons are defined to be bosons in highly occupied momentum states. The average occupancy of the states that give rise to the data in the inset is not so large: at $T^* = 0.50$, just before the suppression transition, the average occupancy per momentum state for states with $\bar{N}_a^{\text{id}}(z) > 1$ is only 6.3. The rate of change of momentum of a condensed boson for a given force is reduced by a factor of the inverse of the occupancy of its state, and hence the contribution to the absence of viscosity in superfluid flow is greatest for condensed bosons in the most highly occupied states (Attard 2025b).

Figure 2 shows the constant volume heat capacity per atom on the liquid saturation curve. In the case where no atoms are excluded from the position permutation loops (open symbols), the heat capacity noticeably increases with decreasing temperature for $T^* \lesssim 0.80$ ($T \lesssim 8.2\text{ K}$ using ε_{He}). However, when the optimum number of bosons are excluded from the position permutation loops, the heat capacity remains rather flat until the inclusion (suppression) transition at $T^* = 0.45$, or $T = 4.6\text{ K}$ using ε_{He} , where it begins to increase sharply. This is the point at which one would first observe the approach to the λ -transition. Between this point and the peak of the heat capacity there are no condensed bosons and hence no superfluidity.

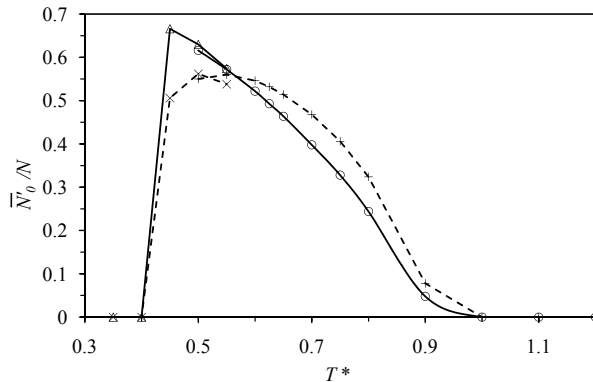


FIG. 3: Most likely fraction of low-lying Lennard-Jones ^4He atoms. Using Eq. (2.21) for pure loops, the circles are from homogeneous simulations and the triangles are from simulations of a droplet. Using Eq. (2.28) including pure loops and mixed chains, the plus symbols are from homogeneous simulations and the times symbols are from simulations of a droplet. The lines connecting symbols are eye guides.

Experimentally, the temperature interval from the minimum to the peak in the measured heat capacity on the high temperature side of the λ -transition is about 0.4 K (Donnelly and Barenghi 1998). This shows the necessity for controlling the growth of position permutation loops in the high temperature regime by excluding the condensed bosons from them. As the filled symbols in Fig. 2 show, this gives a heat capacity approaching the λ -transition that more closely resembles the experimental measurements than otherwise as it reduces the temperature range over which the heat capacity increases and it makes the subsequent increase very sharp. It suggests that the suppression transition should be interpreted as the beginning of the λ -transition proper.

In the constrained free energy at lower temperatures there is no sign of condensation re-emerging or of a peak in the heat capacity. Undoubtedly this is due to the simplicity of the Lennard-Jones model, and the neglect of many body potentials and the commutation function. Likely also the exponential form for the position loop symmetrization function fails in the large loop regime. Therefore the most that the data say is that the λ -transition in Lennard-Jones ^4He lies below $T^* = 0.45$ ($T = 4.6$ K using ε_{He}).

Figure 3 shows the optimum number of condensed bosons that minimise the alternative free energy, Eq. (2.21). These are the bosons in low lying momentum states with negligible kinetic energy that are excluded from the position permutation loops. It can be seen that at high temperatures there are negligible numbers of such bosons. In the interval $T^* \in [0.45, 1.0]$ ($T \in [4.6$ K, 10.2 K] using ε_{He}), the fraction of condensed bosons increases to about 65% with decreasing temperature. At about $T^* = 0.4$ an inclusion transition takes place where it has evidently become favorable to eliminate condensed bosons and to instead include all bosons

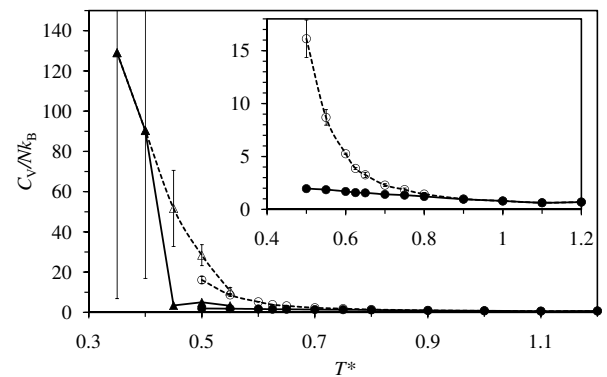


FIG. 4: The specific heat capacity of Lennard-Jones ^4He . The circles are from homogeneous simulations and the triangles from simulations of a droplet. Using Eq. (2.21), the solid symbols have \overline{N}'_0 atoms excluded from the position permutation loops, whereas the open symbols have all atoms included in the loops. The lines connecting symbols are eye guides. The error bars give the 95% confidence level. **Inset.** Magnification at higher temperatures.

in the position permutation loops. The behavior of \overline{N}'_0 shown in the figure is similar to that shown for \overline{N}_{00} in the inset to Fig. 1, although the peak fraction here is about three times higher.

Figure 3 shows that the effect of including mixed chains, Eq. (2.28), is surprisingly small. The peak fraction of condensed bosons is lowered to about 56%, and the inclusion transition is more rounded. The location of the inclusion transition remains unchanged at about 4 K. There is no sign of condensation reemerging due to including these mixed chains.

Figure 4 shows the specific heat capacity that results when \overline{N}'_0 bosons are excluded from the pure position permutation loops. Prior to the inclusion transition there is relatively little increase in the heat capacity. After the transition the heat capacity increases sharply. As mentioned, the experimentally measured width from the peak to the minimum in the heat capacity is about 0.4 K (Donnelly and Barenghi 1998). The empty symbols in Fig. 4, which show the heat capacity if all the bosons participate in position permutation loops, show a significant rise over about 3 K. This may be misleading because because the exponential form for the loop expansion is not reliable when large loops form, which is likely the reason that the constrained free energy does not show any re-emergence of condensation or the peak of the heat capacity. In any case the result show that the mechanism for the divergence of the heat capacity is the formation and growth of position permutation loops, which requires the suppression of condensation.

IV. CONCLUSION

Experimentally we may identify three temperature regimes connected with the λ -transition in ^4He . The first is the high temperature regime, from about 10 K to 2.55 K, in which the heat capacity gradually decreases with decreasing temperature to a local minimum at 2.55 K. The second is the near side of the λ -transition, from 2.55 K to 2.18 K, during which the heat capacity sharply increases and diverges (integrably) to infinity. And the third is the far side of the λ -transition, $T < 2.18$ K, during which the heat capacity decreases, first rapidly and then more gradually. It is only on the far side that superfluidity occurs.

We may interpret these three regimes at the molecular level on the basis of the simulation results for Lennard-Jones ^4He . Although the simplicity of the model fluid and approximations such as the neglect of the commutation function may preclude quantitative accuracy (eg. the saturation density is more than twice the measured value), nevertheless the prediction of the molecular structure ought to be reliable as these reflect the principles of quantum statistical mechanics and the universal attributes of Bose-Einstein condensation.

In the high temperature regime position permutation loops begin to form, and they grow in size and number with decreasing temperature. However, there are also many atoms distant from their nearest neighbors that do not participate in position permutation loops. Condensed atoms begin to occupy the low lying momentum states, with their multiplicity low but increasing with decreasing temperature. In this regime the occupation entropy per atom is marginally greater than the position permutation loop entropy, with on the order of 65% of the ^4He atoms (Fig. 1) being excluded from the position permutation loops (compared to 50% in the high temperature limit). Alternatively 55–60% of the ^4He atoms are in the low lying momentum states (Fig. 3), which is an alternative prerequisite for condensation. These conclusions still hold when mixed permutation chains are included in the analysis. The existence of condensed bosons, which reduce the number of atoms available for position loops, puts a lid on their growth and prevents any noticeable increase in the heat capacity (cf. the filled symbols in the insets to Figs 2 and 4). The reason that there is no superfluidity in this regime is that the occupation of each low lying momentum state is small, being less than about 10, and there being less than about 20% of the atoms in states with an average occupancy greater than unity.

On the near side of the λ -transition, the position permutation loop entropy per atom exceeds the occupation entropy. The minimum in the measured heat capacity marks the suppression transition identified in the simulation data in the text. On the near side of the λ -transition it is more favorable for ^4He atoms to be part of position permutation loops than it is for them to permute with other condensed atoms in the low-lying momentum states, which would exclude them from the position per-

mutation loops. The inclusion of condensed bosons coincides with a rapid growth in size and number of position permutation loops, and a divergence of the heat capacity. This conclusion is unchanged when mixed permutation chains are added, Fig. 3. Because the atoms in the low-lying momentum states do not undergo internal permutations, even in momentum states with high occupancies, there is no superfluidity. (Actually, the results including mixed chains in Fig. 3 indicate that there are no atoms in low-lying momentum states in this regime, which is a more direct way of seeing that there can be no superfluidity.)

I have not directly accessed the far side of the λ -transition in the simulations, and so what follows is somewhat speculative. (But see the appendix added in version 2.) The key challenge is to explain why the λ -transition is marked by an infinite rather than a finite maximum heat capacity. The results in Figs 1 and 3 indicate that on the near side of the λ -transition condensed boons are suppressed, and the results in Figs 2 and 4 indicate that the heat capacity diverges, presumably to infinity. The results in Tables I and II indicate that the two loop series are divergent in this regime. This says that large pure position loops are forming on the near side. (There can be no mixed position chains because there are no condensed bosons to form each head.) Since loops are closed and chains are open, when there is no distinction between condensed and uncondensed bosons there are many more possible chains than loops $g^{(l)} < \tilde{g}^{(l)}$, with the difference growing exponentially with l . At the point of divergence of the pure position loop series, which is presumably the point of infinite heat capacity and the true λ -transition, it becomes favorable for mixed chains to emerge.

The molecular mechanism for this is based on the fact that for any given position configuration and any given permutation, converting an uncondensed boson to a condensed boson increases the weight of the position permutation loop that it is part of by a factor of approximately $e^{\pi\sigma^2/\Lambda^2}$. This is not true for a monomer in the particular permutation, but in this regime no atom will remain a monomer for more than a small minority of permutations. A similar result holds for mixed chains once they emerge, so that long chains are favorably broken into short chains. This appears to be the mechanism by which condensed bosons re-emerge at the peak of the λ -transition and by which their fraction increases with decreasing temperature on the far side of the transition.

The experimental observation is that condensation begins from zero at the λ -transition, as evidenced by the continuity in density and shear viscosity, and the discontinuity in their first temperature derivative. The present explanation for the λ -transition based on the emergence of chains is consistent with that observation in so far as the entropy due to the occupancy of individual momentum states is a collective phenomena, which non-linearity drives the transition. But since occupancy is an intensive variable, it is possible for individual momentum states to become highly occupied for the first

time at the λ -transition, and at the same time the total number of condensed bosons is macroscopically zero. As the temperature is lowered on the far side of the transition, the number of highly occupied momentum states increases such that the fraction of condensed bosons becomes macroscopic.

The reason that the heat capacity decreases as chains replace loops and short chains replace long chains is because of the increasing fraction of condensed bosons, since the ones in low-lying momentum states contribute little to the heat capacity. Also the number of permutation loops and chains has probably maxed out, because large loops and chains block others from forming.

In analyzing pure position permutation loops and mixed chains, the bond weight is a Gaussian with thermal wavelength width. This comes from averaging over momentum states. For the case of uncondensed bosons, changes in momentum state are much more frequent than significant changes in position, and so such averaging is valid. For the case of condensed bosons the rate of change of momentum is inversely proportional to the occupancy of its momentum state, and so it remains in the same momentum state for relatively long periods. Hence it is valid to treat condensed bosons as if they are a separate species.

Superfluidity is due to the permutations between bosons within highly occupied momentum states (Attard 2025b). It should be noted that in arguing above for the emergence of mixed chains on the far side of the λ -transition, in the corresponding symmetrization function, $N_0! [1 + \tilde{g}]^{N_0'}$ (the prefactor would in more precise analysis be replaced by $\prod_a N_a!$), the term unity represents the internal permutations of the individual bosons within each momentum state (ie. independent of the uncondensed bosons in the tail of each chain). Thus the emergence of chains on the far side of the λ -transition is consistent with an increase in the occupation entropy due to internal permutations within momentum states.

On the far side of the λ -transition, the occupancies of the low lying momentum states are larger, presumably many times larger, than they were in the high temperature regime. This means that the occupation entropy is larger due to the internal permutations within each low lying momentum state. It also means that for these condensed atoms the rate of change of momentum is greatly reduced, and that the number of atoms exhibiting such a reduction is greatly increased. These together give rise to superfluidity.

References

Attard P 2002 *Thermodynamics and Statistical Mechanics: Equilibrium by Entropy Maximisation* (London: Academic)

Attard P 2012 *Non-equilibrium thermodynamics and statistical mechanics: Foundations and applications* (Oxford: Oxford University Press)

Attard P 2018 Quantum statistical mechanics in classical phase space. Expressions for the multi-particle density, the average energy, and the virial pressure arXiv:1811.00730

Attard P 2021 *Quantum Statistical Mechanics in Classical Phase Space* (Bristol: IOP Publishing)

Attard P 2025a *Understanding Bose-Einstein Condensation, Superfluidity, and High Temperature Superconductivity* (London: CRC Press)

Attard P 2025b The molecular nature of superfluidity: Viscosity of helium from quantum stochastic molecular dynamics simulations over real trajectories arXiv:2409.19036v5

Le Bellac M, Mortessagne F, and Batrouni G G 2004 *Equilibrium and Non-Equilibrium Statistical Thermodynamics* (Cambridge: Cambridge University Press)

Donnelly R J and Barenghi C F 1998 The observed properties of liquid Helium at the saturated vapor pressure *J. Phys. Chem. Ref. Data* **27** 1217

Einstein A 1924 Quantentheorie des einatomigen idealen gases Sitzungsberichte der Preussischen Akademie der Wissenschaften **XXII** 261

Einstein A 1925 Quantentheorie des einatomigen idealen Gases. Zweite Abhandlung. Sitzungsberichte der Preussischen Akademie der Wissenschaften **I 3**

Lipa J A, Swanson D R, Nissen J A, Chui T C P, and Israelsson U E 1996 Heat capacity and thermal relaxation of bulk helium very near the lambda point *Phys. Rev. Lett.* **76** 944

London F 1938 The λ -phenomenon of liquid helium and the Bose-Einstein degeneracy *Nature* **141** 643

Pathria R K 1972 *Statistical Mechanics* (Oxford: Pergamon Press)

van Sciver S W 2012 *Helium Cryogenics* (New York: Springer 2nd edition)

Tisza L 1938 Transport phenomena in helium II *Nature* **141** 913

Appendix A: Refined Free Energy, Fugacity, and Chains

This appendix extends the text (version 1) in two ways. First it gives a better expression for the free energy and fugacity of the condensed bosons. And second, the mixed position permutation chains are reformulated in order to resolve an inherent contradiction in their treatment in the text. The conclusions in the text are largely unchanged, except that more detail and certainty are provided for the emergence of condensation at and below the λ -transition.

1. Free Energy and Fugacity

In the text the fugacity z , which is required for the condensed boson grand potential, $\Omega_0^{\text{id}}(z, V, T) = \prod_{\mathbf{a}} [1 - ze^{-\beta a^2/2m}]^{-1}$, Eq. (2.9), is determined implicitly by setting $\overline{N}_0^{\text{id}}(z) = N_0$, where $\overline{N}_0^{\text{id}}(z) = \sum_{\mathbf{a}} ze^{-\beta a^2/2m} / [1 - ze^{-\beta a^2/2m}]$ is evaluated numerically by the sum over momentum states for a small system. Here an arguably better approach improves this in two ways.

First, the continuum approximation is made, so that the grand-potential is given by the Bose-Einstein integral (Pathria 1972 Appendix D, Attard 2025 §2.3)

$$\Omega_0^{\text{id}}(\tilde{z}_0, V, T) = -k_B T V \Lambda^{-3} g_{5/2}(\tilde{z}_0), \quad (\text{A.1})$$

and

$$\overline{N}_0^{\text{id}}(\tilde{z}_0) = V \Lambda^{-3} g_{3/2}(\tilde{z}_0). \quad (\text{A.2})$$

For these to be meaningful the condensed boson fugacity must be less than unity, $\tilde{z}_0 < 1$, as is discussed below.

The argument against the continuum approximation in the past has been that it fails to capture the contribution from the ground state bosons (Pathria 1972 §7.1, Attard 2025 §2.3). The basis for this argument is physical rather than mathematical: the maximum ideal boson density that results is less than the measured density of saturated liquid ${}^4\text{He}$. Therefore, it is said, the continuum represents only the excited state bosons, and extra ground state bosons need to be added to make up the discrepancy, $N_0 = N_{4\text{He}}^{\text{meas}} - \overline{N}_*^{\text{id}}(z)$. This has the unfortunate consequence that the fugacity becomes dependent on the system size, which violates the fundamental thermodynamic principle that it is an intensive variable. In fact, however, the problem lies not with the continuum approximation, which is quite accurate (Attard 2025a §2.4), but with the ideal boson model itself. Simply adding the ideal boson ground state to the continuum result compensates for one approximation (the ideal boson model) by introducing another (the added ground state).

In the present approach interactions between bosons are included via the position configuration integral $Q(N, V, T)$, and also via the permutation loops and chains. Thus there is no real reason to follow the ideal gas model and to suppose that the continuum integral only applies to the excited state bosons and that the ground state bosons have to be added separately. Of course the analysis in the text is based on treating condensed and uncondensed bosons as separate species and optimizing their number. The point being made here is that the grand potential of the condensed bosons can be obtained via the continuum integral.

For the second improvement, the fugacity of the condensed bosons is taken to be

$$\tilde{z}_0(N_0) = f_0 \rho \Lambda^3 [1 + \tilde{g}], \quad (\text{A.3})$$

where $\rho = N/V$ is the number density of the liquid (in the results below this is taken to be that of the Lennard-

Jones ${}^4\text{He}$ saturated liquid), and $f_0 = N_0/N$ is the fraction of condensed bosons, which the chain contribution depends upon, $\tilde{g} = \sum_{l=2}^{l_{\text{max}}} f_0 f_*^{l-1} \tilde{g}^{(l)}$, the fraction of uncondensed bosons being $f_* = 1 - f_0$. The part $f_0 \rho \Lambda^3$ is the momentum contribution to the fugacity for ideal bosons, which is augmented with the contribution from the permutation chains. The difference with the text is that this is an explicit expression for the fugacity $\tilde{z}_0(N_0)$ rather than implicit equation to be solved numerically. Of course the consequence is that $\overline{N}_0^{\text{id}}(\tilde{z}_0) \neq N_0$. (These do not have to be equal because the excess contribution from the position configuration integral also contributes.)

One merit of the present expression for the fugacity is that at high temperatures where the chains vanish, $\tilde{g} \rightarrow 0$, it goes over to the ideal boson result. Since in this limit the loops also vanish, $g \rightarrow 0$, the condensed and uncondensed boson are treated identically with the momentum contributions of both being ideal. The interactions for both types of atom are accounted for by the position configuration integral.

With the continuum expression for the condensed boson grand potential, the constrained Helmholtz free energy becomes

$$\begin{aligned} \beta F(N_0|N, V, T) &= -V \Lambda^{-3} g_{5/2}(\tilde{z}_0) + N_0 \ln \tilde{z}_0 + \ln[N_*! \Lambda^{3N_*} V^{N_0}] \\ &\quad - \ln Q(N, V, T) - \sum_{l=2}^{l_{\text{max}}} \frac{N_*^l}{N^{l-1}} g^{(l)}, \end{aligned} \quad (\text{A.4})$$

with $N = N_0 + N_*$ and $z_0(N_0) < 1$. Per atom this is

$$\begin{aligned} \beta F(N_0|N, V, T)/N &= \frac{-1}{\rho \Lambda^3} g_{5/2}(z_0) + f_0 \ln z_0 + f_* \ln[f_* \rho \Lambda^3] - f_* \\ &\quad - \sum_{l=2}^{l_{\text{max}}} f_*^l g^{(l)} + \ln V - N^{-1} \ln Q(N, V, T). \end{aligned} \quad (\text{A.5})$$

Only the terms that depend on f_0 , f_* , and \tilde{z}_0 need to be kept. The optimum fraction of condensed bosons is obtained by minimizing this.

Equivalently, and often more conveniently, one can simply find the zero of the derivative at constant N ,

$$\left(\frac{\partial \beta F(N_0|N, V, T)}{\partial N_0} \right)_N \quad (\text{A.6})$$

$$\begin{aligned} &= \ln \tilde{z}_0 + \left[N_0 - \overline{N}_0^{\text{id}}(\tilde{z}_0) \right] \frac{\partial \tilde{z}_0}{\tilde{z}_0 \partial N_0} - \ln \frac{N_* \Lambda^3}{V} \\ &\quad + \sum_{l=2}^{l_{\text{max}}} l \left(\frac{N_*}{N} \right)^{l-1} g^{(l)}. \end{aligned} \quad (\text{A.7})$$

One has

$$\begin{aligned} \frac{\partial \tilde{z}_0}{\tilde{z}_0 \partial N_0} &= \frac{1}{N f_0 [1 + \tilde{g}]} \left\{ [1 + \tilde{g}] \right. \\ &\quad \left. + f_0 \sum_{l=2}^{l_{\text{max}}} [f_*^{l-1} - (l-1) f_0 f_*^{l-2}] \tilde{g}^{(l)} \right\}. \end{aligned} \quad (\text{A.8})$$

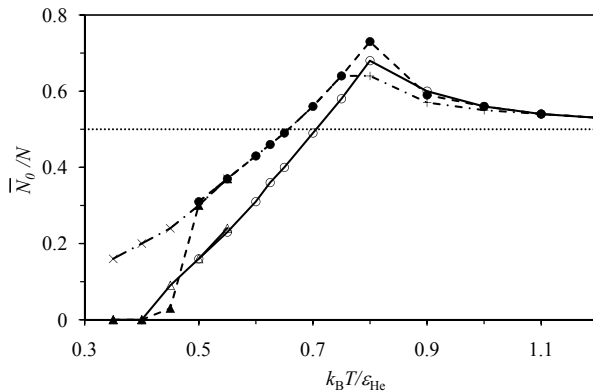


FIG. 5: Most likely fraction of condensed Lennard-Jones ^4He atoms. The circles are from a homogeneous liquid (periodic boundary conditions) and the triangles are from simulations of a droplet. The empty symbols are for position loops and chains, and the filled symbols are for position loops only. The algebraic symbols are from Eq. (A.10). The dotted line and the lines connecting the symbols are eye guides. Note that $\epsilon_{\text{He}}/k_B = 10.22$ K.

Since $\bar{N}_0^{\text{id}}(\tilde{z}_0) \sim N_0[1 + \tilde{g}]$, $N_0 \rightarrow 0$, it follows that $\lim_{N_0 \rightarrow 0} [N_0 - \bar{N}_0^{\text{id}}(\tilde{z}_0)] \partial \tilde{z}_0 / \tilde{z}_0 \partial N_0 \rightarrow 0$, $N_0 \rightarrow 0$.

As mentioned above these expression are only meaningful for $\tilde{z}_0 < 1$, which is guaranteed for low condensed boson fractions, specifically for $f_0 = 0$. At higher fractions and lower temperatures, \tilde{g} becomes large and this condition is violated. The numerical results (next) for the optimum fraction \bar{f}_0 satisfy this condition. At those temperatures where not all fractions are valid, \bar{f}_0 gives the lowest free energy, usually at a boundary of the valid range (or ranges), where the derivative does not vanish.

Figure 5 shows the optimum fraction of condensed bosons with (empty symbols) and without (filled symbols) the chain contribution. At high temperatures the loops and chains are negligible, and the optimum fraction approaches 50% as there is nothing to distinguish condensed from uncondensed bosons in this regime. Because of this the nomenclature ‘condensed’ is a little misleading. As the temperature is decreased, the optimum fraction of condensed bosons first rises slowly above 50%, and then abruptly begins to fall. Compared to the results in the text, specifically Fig. 1, the decrease in the fraction of condensed bosons with decreasing temperature is more gradual here, and it begins at a higher temperature. Including the chains gives a lower fraction of condensed bosons, and a more gradual fall to zero condensation toward the end of the temperature range shown. In both cases condensation is completely suppressed at the lowest temperatures studied. There is quite good agreement between the simulation results for the homogeneous liquid (circles) and the droplet in equilibrium with its own vapor (triangles) where their temperature range overlaps.

The first temperature at which $\tilde{z}_0(N_0) > 1$ is $T^* = 0.90$, namely at the constrained fraction $f_0 = 0.93$ (with chains) or $f_0 = 0.94$ (without chains). (These are not the

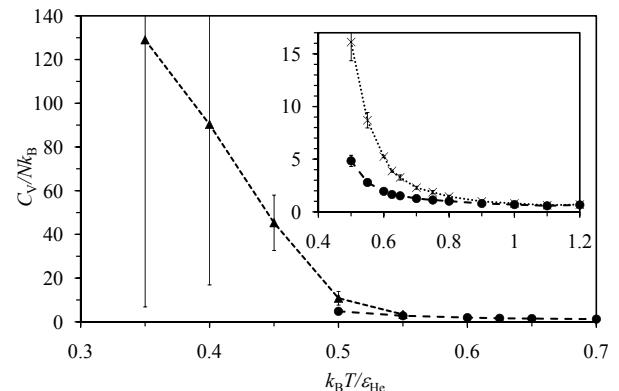


FIG. 6: The specific heat capacity of Lennard-Jones ^4He due to the classical contribution plus position loops only. The circles are from a homogeneous liquid and the triangles are from simulations of a droplet. The filled symbols have the \bar{N}_0 condensed atoms excluded from the position permutation loops, whereas the crosses in the inset have all atoms included in the position loops. The lines connecting symbols are eye guides. The error bars gives the 95% confidence level.

optimum fraction.) This constrained fraction decreases with decreasing temperature. Temperatures above the cusp at $T^* = 0.80$ evident in Fig. 5 have the minimum in the free energy located within the domain $\tilde{z}_0(N_0) < 1$, whereas for temperature at and below this cusp the minimum occurs at the boundary of the valid domain.

Also shown in Fig. 5 are the results of the free energy Eq. (A.10), which includes the chain grand potential similarly to the loops (see below). The results are rather similar to the results without chains, except that they don’t jump to zero condensed boson fraction at the lowest temperatures.

Figure 6 shows the specific heat capacity at constant volume. No contribution from the mixed permutation chains is included here. There is a sharp increase in the specific heat capacity for $T^* \lesssim 0.5$ ($T \lesssim 5.11$ K). This corresponds to the regime in which condensation is suppressed and all atoms are therefore included in the position permutation loops. This divergence in the heat capacity is due to the divergence of the position permutation loop series. It can be seen in the inset that the non-zero number of condensed bosons, and their exclusion from the position permutation loops for $T^* \gtrsim 0.5$ significantly reduces and flattens the heat capacity compared to if all atoms had participated in the position permutation loops. This has the effect of sharpening the high temperature side of the λ -transition. Again the differences with the results in the text are quantitative rather than qualitative.

The Lennard-Jones saturation liquid density is about 2.7 times the measured density. This causes the parameter $\rho \Lambda^3$ to be overestimated, as well as the peak of the pair distribution function. These are the reasons that the heat capacity diverges at a higher temperature in the Lennard-Jones liquid than measured in ^4He .

2. Permutation Chain Grand Potential

In the preceding section the condensed bosons are ‘dressed’ with the mixed chains with which they are associated, which gives rise to the effective fugacity $\tilde{z}_0 = z_0^{\text{id,cl}}[1+\tilde{g}]$. An alternative approach is to treat the chains similarly to the loops by defining the chain grand potential. The justification for this may be illustrated by the double dimer permutation,

$$\begin{aligned} \eta^{(2,2)}(\mathbf{T}) &= \sum_{j < k} \sum_{l,m}^{N_0, N_*} (l \neq m) e^{-\mathbf{p}_l \cdot \mathbf{q}_{lj}/i\hbar} e^{-\mathbf{p}_m \cdot \mathbf{q}_{mk}/i\hbar} \\ &\approx \frac{1}{2} \sum_{j=1}^{N_0} \sum_{l=1}^{N_*} e^{-\mathbf{p}_l \cdot \mathbf{q}_{lj}/i\hbar} \sum_{k=1}^{N_0} \sum_{m=1}^{N_*} e^{-\mathbf{p}_m \cdot \mathbf{q}_{mk}/i\hbar} \\ &= \frac{1}{2} \eta^{(2)}(\mathbf{T})^2. \end{aligned} \quad (\text{A.9})$$

Dropping the restriction $l \neq m$ gives negligible error in the thermodynamic limit. The factor of one half obviously represents the second term in an infinite exponential series of products that can be extended to all chain lengths, just as for position permutation loops (Attard 2018, 2021, 2025a §7.3.3).

The corresponding Helmholtz free energy is given by

$$\begin{aligned} \beta F(N_0, N_*, V, T) & \quad (\text{A.10}) \\ &= \Omega_0(z_0, V, T) + N_0 \ln z_0 + \ln[N_*! \Lambda^{3N_*} V^{-N_*}] \\ &\quad - \ln[Q(N, V, T)/V^N] - Ng(f_*) - N\tilde{g}(f_0, f_*), \end{aligned}$$

where $g(f_*) = \sum_l f_*^l g^{(l)}$ and $\tilde{g}(f_0, f_*) = \sum_l f_0 f_*^{l-1} \tilde{g}^{(l)}$. With $z_0 = f_0 \rho \Lambda^3$, the derivative at constant N is

$$\begin{aligned} \frac{\beta}{N} \frac{\partial F(N_0, N_*, V, T)}{\partial f_0} & \quad (\text{A.11}) \\ &= \ln z_0 + [1 - z_0^{-1} g_{3/2}(z_0)] - \ln[f_* \rho \Lambda^3] \\ &\quad + \sum_{l=2}^{l_{\max}} l f_*^{l-1} g^{(l)} - \sum_{l=2}^{l_{\max}} [f_*^{l-1} - (l-1) f_0 f_*^{l-2}] \tilde{g}^{(l)}. \end{aligned}$$

The results in Fig. 5 show that this alternative free energy expression is not significantly different to that given in the preceding section. Perhaps the most noticeable difference is that condensation is partially but not entirely suppressed at the lowest temperatures shown. One should be cautious about the conclusions drawn from these free energy expressions because of their approximate nature, the simplicity of the Lennard-Jones model, and the limited number of terms that are used in the loop and chain series.

3. Summary

The author’s present understanding of the λ -transition may be summarized as:

1. On the high temperature side of the λ -transition position permutation loops form. The links have Gaussian weight dependent upon the bond length, $e^{-\pi q_{j_k, j_{k+1}}^2 / \Lambda^2}$, where the thermal wavelength Λ comes from the momentum integration with Maxwell-Boltzmann weight, $e^{-\beta p_{j_k}^2 / 2m}$. There are few condensed bosons in this regime because there are many more accessible momentum states than there are atoms.
2. As the temperature is decreased, the driving force for condensed bosons (ie. those in multiply occupied low-lying momentum states) increases. This is due (1) to the fewer available momentum states, (2) the occupation entropy of multiply occupied states, and (3) the chain entropy.
3. Chains begin as loops but with a longer bond connecting the condensed boson (the head) with the adjacent non-condensed boson (the tail). The longer bond arises from the greater weight given to low-lying momentum states than the Maxwell-Boltzmann weight alone. The average end-to-end distance of a chain decreases with increasing momentum state of the condensed boson.
4. Bosons in the same momentum state, which in practice means the condensed bosons in multiply occupied low-lying momentum states, are permuted non-locally independently of any chain that they can also form. These non-local permutations and the consequent occupation entropy give rise to superfluidity.
5. Chains occur below the λ -transition, as experimentally evidenced by the decrease in density and the decrease in the specific heat capacity. Because chains are less compact than loops the density decreases below the λ -transition. Because condensation leads to shorter chains and fewer loops, and because a condensed boson has less energy than an uncondensed boson, the heat capacity decreases.